

1 Article

# 2 Biodiesel production (FAEEs) by heterogeneous 3 combi-lipase biocatalysis using wet extracted lipids 4 from microalgae

5 Alejandra Sánchez-Bayo <sup>1</sup>, Victoria Morales <sup>2</sup>, Rosalía Rodríguez <sup>1</sup>, Gemma Vicente <sup>1</sup> and Luis  
6 Fernando Bautista <sup>2,\*</sup>

7 <sup>1</sup> Department of Chemical, Energy and Mechanical Technology. ESCET, Universidad Rey Juan Carlos, 28933,  
8 Móstoles, Madrid, Spain; alejandra.sanchezbayo@urjc.es (ASB), rosalia.rodriguez@urjc.es (RR),  
9 gemma.vicente@urjc.es (GV)

10 <sup>2</sup> Department of Chemical and Environmental Technology. ESCET, Universidad Rey Juan Carlos, 28933,  
11 Móstoles, Madrid, Spain; victoria.morales@urjc.es (VM), fernando.bautista@urjc.es (FB)

12 \* Correspondence: fernando.bautista@urjc.es (FB); Tel.: +34-914-888-501

13

14 **Abstract:** The production of fatty acids ethyl esters (FAEEs) to be used as biodiesel from oleaginous  
15 microalgae shows great opportunities as an attractive source for the production of renewable fuels  
16 without competing with human food. To ensure the economic viability and environmental  
17 sustainability of the microbial biomass as a raw material, the integration of its production and  
18 transformation into the biorefinery concept is required. In the present work, lipids from wet *Isochrysis*  
19 *galbana* microalga were extracted with ethyl acetate with and without drying the microalgal biomass  
20 (dry and wet extraction method, respectively). Then, FAEEs were produced by lipase-catalyzed  
21 transesterification and esterification of the extracted lipids with ethanol using lipase B from *Candida*  
22 *antarctica* (CALB) and *Pseudomonas cepacia* (PC) lipase supported on SBA-15 mesoporous silica  
23 functionalized with amino groups. The conversion to FAEEs with CALB (97 and 85.5 mol% for dry  
24 and wet extraction, respectively) and PS (91 and 87 mol%) biocatalysts reached higher values than  
25 those obtained with commercial Novozym 435 (75 and 69.5 mol%). Due to the heterogeneous nature  
26 of the composition of microalgae lipids, mixtures with different CALB:PC biocatalyst ratio were used  
27 to improve conversion of wet-extracted lipids. The results showed that a 25:75 combi-lipase produced  
28 a significantly higher conversion to FAEEs (97.2 mol%) than those produced by each biocatalyst  
29 independently from wet-extracted lipids and similar ones than those obtained by each lipase from  
30 the dry extraction method. Therefore, that optimised combi-lipase biocatalyst, along with achieving  
31 the highest conversion to FAEEs, would allow improving viability of a biorefinery since biodiesel  
32 production could be performed without the energy-intensive step of biomass drying.

33 **Keywords:** FAEEs, biodiesel, mixed biocatalysts, lipases, microalgae.

34

## 35 1. Introduction

36 Nowadays, we are facing a major energy crisis not only caused by the decline of fossil reserves  
37 but also by the problems caused by their use. Therefore, there is a need to look for new sources of  
38 cleaner, safer and renewable energy. Currently, the research is focuses in obtaining advanced biofuels

39 to ensure the economic viability and environmental sustainability of biomass as a raw material<sup>1</sup>.  
40 Oleaginous microalga are promising species that can accumulate large amount of lipids (> 20 wt% of  
41 their biomass). They constitute an attractive source for the production of biofuels such as biodiesel  
42 without competing with human food<sup>2</sup>.

43 Biodiesel can be generated from microalga oil that is esterified or transesterified with methanol  
44 or ethanol into methyl or ethyl esters of fatty acids (FAMEs or FAEEs, respectively) in the presence  
45 of a catalyst. Due to its high content of free fatty acids, the most common way to carry out the  
46 transesterification and esterification reactions of the lipids extracted from microalgae is by using acid  
47 catalysts. This generates certain disadvantages not only in the process, such as high energy  
48 consumption, corrosion of materials and the difficulty of transesterifying triglycerides, but also in the  
49 post-reaction treatments, such as the recovery of the catalyst<sup>3</sup>. In recent years, new catalysts based  
50 on enzymes (biocatalysts) are being developed to avoid these problems<sup>4</sup>, achieving better selectivity  
51 and specificity. Immobilised lipases can be an alternative because they are capable of carrying out the  
52 transesterification and esterification reactions at lower temperatures energy cost, facilitating the  
53 recovery of the catalyst and the purification of glycerol<sup>5</sup>. However, the main problem of biocatalysts  
54 is the presence of water in the reaction medium that can cause the hydrolysis of esters. In addition,  
55 the use of certain solvents such as methanol can lead to inactivation of the catalyst<sup>6,7</sup>.

56 Due to the high cost of enzymes, the use of heterogeneous biocatalysts is required for the  
57 economic viability of the whole process since they can be reused. In addition, the immobilization of  
58 enzymes in solid carriers can increase thermal and chemical stability and protects enzyme molecules  
59 from denaturation. There are different techniques of enzymatic immobilization: binding to the  
60 support, confinement or encapsulation and cross-linking<sup>8</sup>. The most common technique is to bind the  
61 enzyme onto the support by covalent or ionic attachment or by physical adsorption<sup>9</sup>. To carry out  
62 this immobilization, materials such as mesoporous silicas (SBA-15, SBA-16, MCM-41, FDU-12)<sup>10-14</sup> or  
63 carbon nanotubes<sup>15,16</sup> have been used. The above materials have large pores or cavities where the  
64 enzymes can be housed. However, it is usually necessary to modify the surface of support to achieve  
65 a better anchorage by functionalization with amine, chloride, sulfur or phenol groups<sup>10,14,17-20</sup>.

66 Because of the high specificity of lipases for different substrates, catalytic activity of lipases  
67 depends on the source organism producing the enzyme. Most of biodiesel production from  
68 microalgal oil has been done with lipases from *Pseudomonas cepacia*<sup>16,21</sup>, *P. fluorescens*<sup>16,22</sup>, *Thermomyces*  
69 *lanuginosus*<sup>16,23</sup>, *Candida rugosa*<sup>16,24</sup> and *C. antarctica*<sup>11,16</sup>. The last one is frequently used in the form of  
70 the commercial catalyst Novozym 435<sup>6,16,25,26</sup>. Although most of studies reported the use of single  
71 lipases, some authors showed that the yield of FAEE could increase when some lipases are used in  
72 combination<sup>5,21</sup>. Therefore, the concept of combi-lipase biocatalysts have been recently developed to  
73 improve the biodiesel production processes<sup>27-29</sup>. However, the previous studies using combi-lipase  
74 systems used oils from vegetable crops such as palm, soybean or coffee, but they did not used the  
75 more complex microalgal oil as a source for biodiesel.

76 In this work, biodiesel (FAEEs) were produced using enzymatic catalysts from lipids extracted  
77 with ethyl acetate from both wet and dry biomass from microalgae. For this purpose, two enzymes  
78 from different origin were assessed: lipase B from the fungus *Candida antarctica* (CalB) and lipase  
79 from the bacterium *Pseudomonas cepacia* (PC) which were supported on amino-functionalized SBA-  
80 15. The results were compared to those obtained with the commercial Novozym 435<sup>®</sup> catalyst. In

81 addition, both enzymes were combined in different proportions to evaluate the synergistic activity  
82 and selectivity towards biodiesel production.

## 83 2. Results and Discussions

### 84 2.1. Characterization of the synthesized enzymatic catalyst

85 This section contains the most relevant results of the synthesis of the mesoporous silica material  
86 SBA-15 as well as the modifications thereof when incorporating amino groups, glutaraldehyde and  
87 the enzymes.

88 The textural properties are shown in Table 1. The pore surface and diameter are reduced slightly  
89 after functionalization of the surface with amino groups and further glutaraldehyde linkage as  
90 spacer-arm to favor the subsequent binding of the enzyme. Before functionalization, pore size of SBA-  
91 15 was 59.6 Å, and the surface area was the largest, 847.2 m<sup>2</sup>/g, which decreased to 46.3 Å and 841.8  
92 m<sup>2</sup>/g, respectively, as chain length increased after amine group and glutaraldehyde introduction <sup>30</sup>.  
93 However, pore volume and surface area were drastically reduced with the introduction of enzymes,  
94 both properties decreasing by ~70% with respect to the original SBA-15.

95 **Table 1.** Textural properties and enzyme fixed with synthesized mesoporous materials.

Material	S <sub>BET</sub> (m <sup>2</sup> /g) <sup>1</sup>	D <sub>P</sub> (Å) <sup>2</sup>	V <sub>P</sub> (cm <sup>3</sup> /g) <sup>3</sup>	Protein/material (mg/g)
SBA-15	847.3	59.6	1.307	-
SBA-15-NH <sub>2</sub>	843.2	58.5	1.233	-
SBA-15-NH <sub>2</sub> G	841.8	56.3	1.186	-
SBA-15-NH <sub>2</sub> G-PC	275.4	55.0	0.378	35
SBA-15-NH <sub>2</sub> G-CalB	262.3	56.2	0.393	33

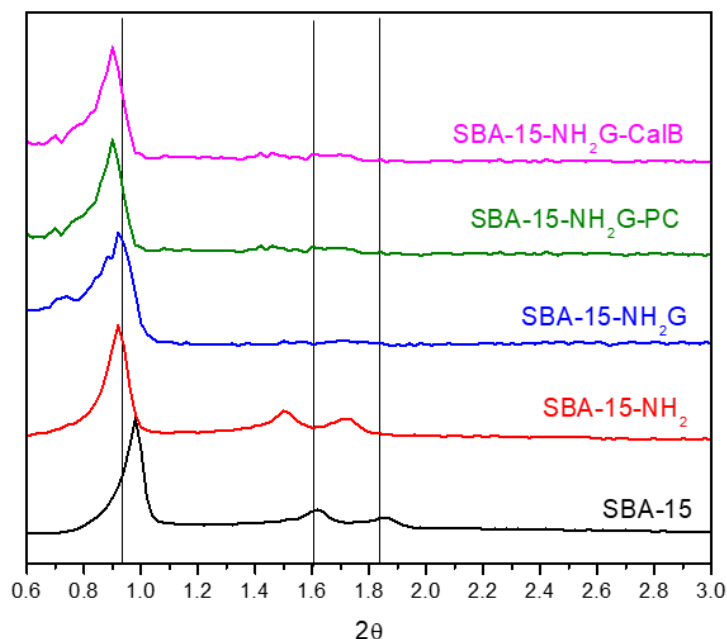
96 <sup>1</sup> BET surface area, <sup>2</sup> BJH pore diameter, <sup>3</sup> Pore volume at P/P<sub>0</sub> = 0.95.

97 The amount of enzyme loaded in each biocatalyst was determined by mass balance measuring  
98 the enzyme concentration in the supernatant solution using the Bradford's assay. The immobilization  
99 values were 35 and 33 mg/g for SBA-15-NH<sub>2</sub>G-PC and SBA-15-NH<sub>2</sub>G-CalB, respectively, similar to  
100 those obtained by Bautista et al.<sup>4</sup> (36.1 mg/g) and slightly lower than that obtained by Serra et al. (44  
101 mg/g) <sup>31</sup>, both using CalB as enzyme. The slighting higher incorporation enzyme in the case of PC  
102 may be due to the fact that its size is somewhat smaller (3 × 3.2 × 6.6 nm)<sup>32</sup> and can enter into the pores  
103 more easily than CalB (3 × 4 × 6 nm)<sup>33</sup>.

104 Regarding the structure, XRD (Figure 1) shows three reflection peaks at 2θ=0.97°, 1.6° and 1.9°  
105 corresponding to *p6mm* mesoporous hexagonal symmetry (planes (100), (110) and (200),  
106 respectively)<sup>34</sup>. Based on the results obtained, the immobilization of enzymes covalently bound to the  
107 material does not modify its structure<sup>10</sup>.

108 Figure 2 shows TEM images obtained from SBA-15 (a) and modified material with anchored  
109 lipases from PC (b) and CalB (c). It is clearly noted that both samples show the arrays of long-range  
110 mesopore channels, which are similar to the image of SBA-15 reported in the literature<sup>20</sup>. When the  
111 SBA-15 contains enzymes partially occupying the interior of its pores, it can appreciated with the  
112 different degrees of sharpness of the channels, a morphology similar to that observed by Mohammadi  
113 et al.<sup>35</sup>. However, as explained by Abdullah et al.<sup>12</sup>, the fact that the modification of the surface of the

114 SBA-15 material was made by grafting, a posteriori, prevents major structural changes from taking  
 115 place and only intervening in the formation of new links with Si-O-Si that are on the surface.

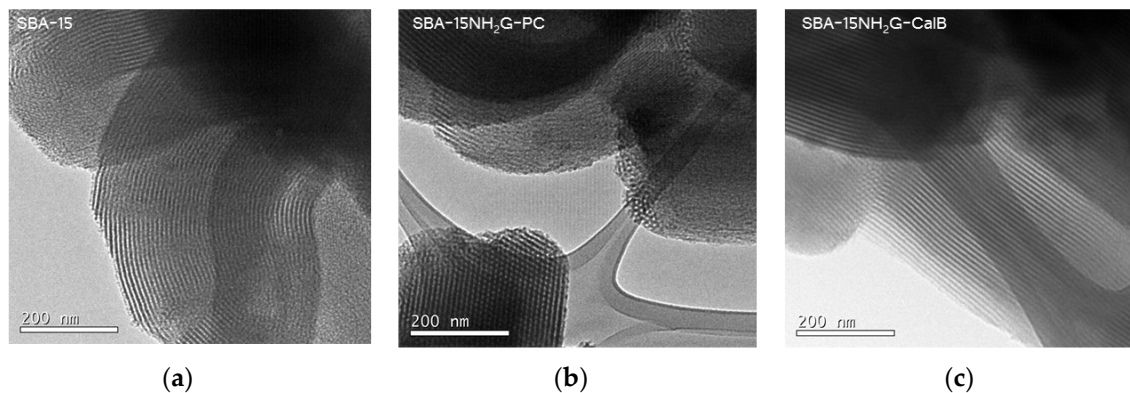


116

117

**Figure 1.** X-ray diffractograms of the mesoporous materials.

118



(a)

(b)

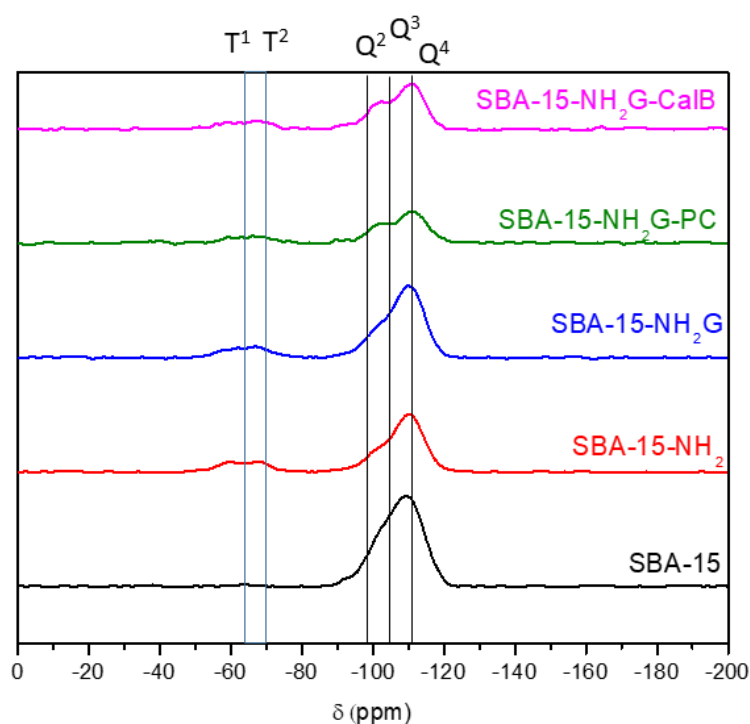
(c)

119

**Figure 2.** TEM micrographs: (a) SBA-15, (b) SBA-15-NH<sub>2</sub>G-PC, (c) SBA-15-NH<sub>2</sub>G-CalB.

120 The <sup>29</sup>Si NMR spectrum (Figure 3) of pure silica shows one wide signal within the range -90 to -110  
 121 ppm that correspond to the Si(OSi)<sub>4</sub> (Q<sup>4</sup>), HOSi(OSi)<sub>3</sub> (Q<sup>3</sup>) and (HO)<sub>2</sub>Si(OSi)<sub>2</sub> (Q<sup>2</sup>) sites of the silica  
 122 framework<sup>36</sup>. Around a displacement -60 to -78 ppm, a broad signal can be seen that corresponds to  
 123 two signals created by the Si-C links corresponding to RSi(OSi)<sub>3</sub> (T<sup>3</sup>) and RSi(HO)(OSi)<sub>2</sub> (T<sup>2</sup>)<sup>37</sup>. These  
 124 last two signals are due to the incorporation of the organic part (CH<sub>3</sub>CH<sub>2</sub>CH<sub>2</sub>NH<sub>2</sub>) by linking on the  
 125 surface of the material. The peak areas were calculated after Gaussian deconvolution of the spectra  
 126 considering the associated species and the respective intensities. The results of the integrations  
 127 (Table 2) show that the greatest contribution to the areas is given by the peak corresponding to a Si  
 128 atom linked to four Si-O structures, i.e., corresponding to the Q<sup>4</sup> signal. Overlapped with this peak,  
 129 two signals of smaller area corresponding to the formation of one or two Si-OH bonds, signals Q<sup>3</sup>  
 130 and Q<sup>2</sup> respectively. The T signals appear when the surface of the material is modified with the

131 previously mentioned organic group and can be observed in the spectrum into overlapping signals  
 132 of areas similar one each other. These results confirm that the structure is not modified when both  
 133 organic modifiers and lipases are introduced<sup>38</sup>.



134

135

**Figure 3.** <sup>29</sup>Si NMR spectra of the different materials.

136

**Table 2.** Relative peak area in the NMR-<sup>29</sup>Si spectra

Material	Q <sup>4</sup> (%)	Q <sup>3</sup> (%)	Q <sup>2</sup> (%)	T <sup>3</sup> (%)	T <sup>2</sup> (%)
SBA-15	83.8	13.4	2.77	-	-
SBA-15-NH <sub>2</sub>	66	10.2	3.42	10.32	10.23
SBA-15-NH <sub>2</sub> G	64.5	13.4	2.41	9.78	9.93
SBA-15-NH <sub>2</sub> G-PC	68.5	7.9	2.8	10.76	9.96
SBA-15-NH <sub>2</sub> G-CalB	63.9	7.8	2.49	11.87	12.21

137

138

139

140

141

142

143

144

145

146

147

148

149

The elemental analysis shows how the composition of hydrogen, carbon, nitrogen and oxygen varies as new functional groups, amino and aldehyde are introduced into the structure, as well as with the incorporation of enzymes. The results shown in Table 3 are coherent since the initial mesoporous structure contains only silicon and hydrogen. The presence of nitrogen, carbon and oxygen are due to the incorporation of the different functional groups in the SBA-15. The introduction of the amino group from APTES increases the nitrogen concentration to ~2.8%, but the incorporation of glutaraldehyde decreases the nitrogen content to 2.2%, due to the presence of carbon, hydrogen and oxygen into the structure. Similar results are reported previously for different functionalization of SBA-15 materials<sup>19</sup>. Conversely, an increase of all the elements is observed after lipase immobilisation in SBA-15NH<sub>2</sub>G-PC and SBA-15NH<sub>2</sub>G-CalB because the incorporation of the lipase molecules added N, C and H, as expected.

150

**Table 3.** Elemental analysis of synthesized mesoporous materials

Material	N (%)	C (%)	H (%)	S (%)
SBA-15	0.00±0.00	0.00±0.00	0.19±0.01	n.d.
SBA-15NH <sub>2</sub>	2.77±0.01	8.01±0.04	1.97±0.02	n.d.
SBA-15NH <sub>2</sub> G	2.2±0.1	15.1±0.5	2.23±0.09	n.d.
SBA-15NH <sub>2</sub> G-PC	2.59±0.02	16.8±0.2	2.71±0.04	n.d.
SBA-15NH <sub>2</sub> G-CalB	2.49±0.01	21.07±0.02	3.28±0.02	0.01±0.01

151

n.d.: not detected (lower than the detection limit)

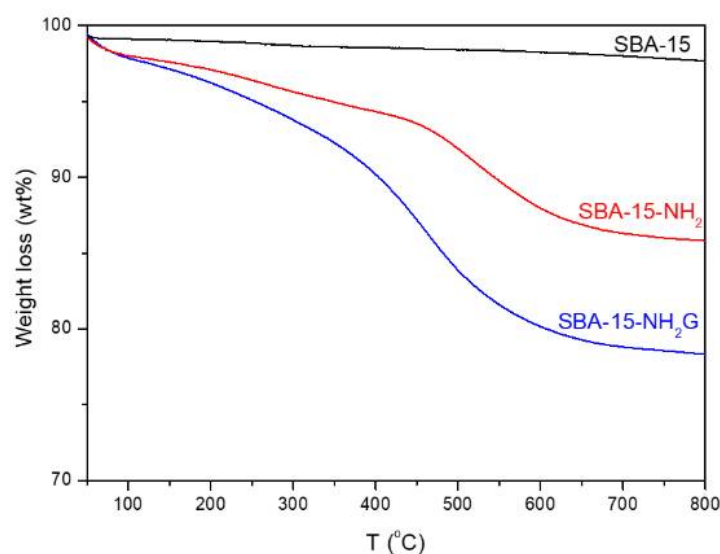
152

After water removal at  $T < 100^\circ\text{C}$ , thermogravimetric analysis shows a weight loss between 200 and 300°C that corresponds to glutaraldehyde followed by the loss of the amino group at temperatures between 300 and 600°C (Figure 4). The results of this analysis show an organic loss, corresponding to propylamine ( $\text{CH}_3\text{CH}_2\text{CH}_2\text{NH}_2$ ), of 11.8 wt% in all the materials. The nitrogen content present in the material SBA-15-NH<sub>2</sub> according to this test (2.8 wt%) corroborates the results of elemental analysis obtained (Table 3).

158

A weight loss of 7.48% is observed in the material SBA-15-NH<sub>2</sub>G, which implies an incorporation of glutaraldehyde in 37 wt% with respect to the amount of available amino groups. This indicates that part of amino groups incorporated into the material did not form bonds with glutaraldehyde. In addition, this test has allowed to corroborate the results of nitrogen content (2.35 wt%) with that obtained by elemental analysis (2.23 wt%).

162



163

164

**Figure 4.** Thermogravimetric analysis of SBA-15 and functionalized materials.

165

## 2.2. Production of FAEEs using single lipase biocatalysts

166

The activity of both synthesized biocatalysts (SBA-15-NH<sub>2</sub>G-CalB and SBA-15-NH<sub>2</sub>G-PC) towards FAEEs production from wet and dry extracted lipids from *I. galbana* was evaluated and compared with the commercial Novozym 435. The results were assessed based on the molar conversion of saponifiable lipids measured by <sup>1</sup>H NMR (Table 4). As it can be seen, the lipid extraction method had a large impact on lipase-catalysed conversion to FAEEs. When the microalgal oil, used as feedstock, was extracted by the wet method, the results showed a reduction in FAEEs production

171

172 from 97 to 85.5 mol% and from 91 to 87 mol% using CalB and PC lipase-based biocatalysts,  
 173 respectively. The commercial Novozym 435 also showed a negative effect when lipids extracted by  
 174 the wet method was used. Microalgal oils from both the wet and dry extraction methods did not  
 175 contain water. Therefore, the decrease in conversion may be caused by the extraction of water-soluble  
 176 lipase-inhibitor compounds during the wet route that are not present in the oil extracted from dry  
 177 biomass, because lipase activity it is negatively affected by polar compounds that can cause inhibition  
 178 or denaturation <sup>39</sup>.

179

**Table 4.** Conversion to FAEEs using single lipases

Lipid extraction method	Catalyst	Conversion (mol%)
Dry	<i>CalB</i>	97±1
	<i>PC</i>	91±2
	<i>N435</i>	75±2
Wet	<i>CalB</i>	85.5±0.8
	<i>PC</i>	87±2
	<i>N435</i>	69.5±0.6

180

181 The highest conversion to FAEEs (97 mol%) using dry extracted lipids with ethyl acetate from *I.*  
 182 *galbana* microalgae was achieved using SBA-15-NH<sub>2</sub>G-CalB as biocatalyst. For the wet extraction  
 183 route, both CalB and PC lipase-based biocatalysts showed similar activity (85.5 and 87 mol%,  
 184 respectively) so that SBA-15-NH<sub>2</sub>G-CalB seems to be more sensitive to the presence of water or other  
 185 polar compounds likely extracted during the wet process. However, in all cases, the synthesised  
 186 biocatalysts SBA-15-NH<sub>2</sub>G-CalB and SBA-15-NH<sub>2</sub>G-PC were significantly more active towards  
 187 FAEEs production than the commercial Novozym 435, proving the better performance of both  
 188 biocatalysts synthesised in the present work.

### 189 2.3. Production of FAEEs using combi-lipase biocatalysts

190 In recent years, the search for new biocatalysts calls for the combination of different enzymes of  
 191 different specificity to produce a higher production yield of FAEEs<sup>27,40</sup>. Consequently, a biocatalyst  
 192 formed by the combination in different proportions of CalB and PC supported on SBA-15 modified  
 193 with amino groups and glutaraldehyde is used in order to evaluate the FAEEs production in the same  
 194 conditions used previously, using the lipids extracted by wet route with ethyl acetate as raw material.

195

**Table 5.** Conversion to FAEEs using combi-lipases.

CalB:PC lipase ratio	Conversion (mol%)
0:100	87±2
25:75	97.2±0.5
50:50	81±2
75:25	89.7±0.3
100:0	85.0±0.8

196

197 Table 5 shows the synergistic effect of different combi-lipases on the conversion to FAEEs, along  
 198 with those values achieves with the corresponding single-lipase biocatalysts It is observed that the

199 combi-lipase 25:75 produced the highest conversion to FAEs (97.2 mol%) which is more than 10%  
 200 higher than biocatalysts formed by CalB or PC alone. This is a remarkable result because it  
 201 demonstrates that it is possible to design a catalyst that contains an optimized mixture of different  
 202 lipases that maximizes the conversion to FAEs.

203 **Table 6.** Fatty acid profile of FAEs obtained with combi-lipase 25:75 SBA-15-NH<sub>2</sub>G-CalB:SBA-15-NH<sub>2</sub>G-PC.

Fatty acid		Composition (%)
Myristic	C14:0	9.0
Palmitic	C16:0	11.3
Palmitoleic	C16:1	3.6
Stearic	C18:0	0.6
Oleic	C18:1	14.5
Linoleic	C18:2	5.1
Linolenic	C18:3	20.2
Arachidic	C20:0	0.5
Behenic	C22:0	18.2
Erucic	C22:1	0.2
Lignoceric	C24:0	16.8
Saturated		56.3
Monounsaturated		18.3
Polyunsaturated		25.4

204  
 205 The fatty acid profile of FAEs produced by the optimised 25:75 SBA-15-NH<sub>2</sub>G-CalB:SBA-15-  
 206 NH<sub>2</sub>G-PC is shown in Table 6. The major saturated fatty acids are myristic (C14:0) and palmitic  
 207 (C16:0) while palmitoleic (C16:1) and oleic (C18:1) acids represented the main monounsaturated and  
 208 linolenic (C18:3) the most abundant polyunsaturated fatty acid. It is important to highlight the value  
 209 of linolenic acid (20.2%), a concentration about 10% higher than that regulated by EN 14214 standard  
 210 (Table 7). This would require further actions after biodiesel production, such as mixing with biodiesel  
 211 from other lipid sources whose linolenic acid content is lower than that of the microalgae used in this  
 212 work, to meet the required specifications

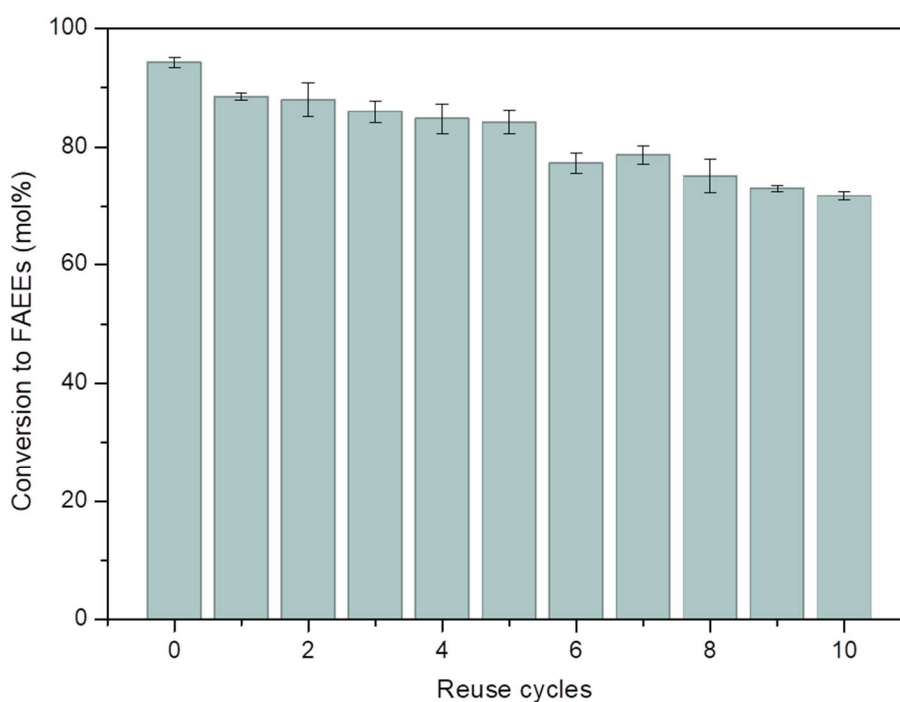
213 **Table 7.** Biodiesel properties obtained by the combi-lipase 25:75 SBA-15-NH<sub>2</sub>G-CalB:SBA-15-NH<sub>2</sub>G-PC

Property	EN 14214	Combi-lipase 25:75
Iodine value (g I <sub>2</sub> / 100 g)	<120	72
Group I metals (Na, K) (mg/kg)	<5	179.1
Group II metals (Ca, Mg) (mg/kg)	<5	205.1
Phosphorous (mg/kg)	<10.0	250.6
Sulfur (mg/kg)	<10	0
Monoglycerides (%)	<0.7	0.6
Diglycerides (%)	<0.2	<0.1
Triglycerides (%)	<0.2	<0.1
Linolenic esters (%)	<12	20.2

214 Other key properties of the biodiesel produced by the combi-lipase biocatalyst 25:75 SBA-15-  
215 NH<sub>2</sub>G-CalB:SBA-15-NH<sub>2</sub>G-PC using the lipids obtained after wet extraction with ethyl acetate are  
216 shown in Table 7. Iodine value as well as mono, di and triglyceride content and sulfur content fulfill  
217 the European standard EN 14214. However, metals and phosphorus content are higher than those  
218 regulated by the above standard, which would require a further purification stage.

#### 219 2.4. Study of the reuse of the heterogeneous enzymatic catalyst

220 As previously mentioned, one of the key features of heterogeneous catalysts for their economic  
221 viability is their possible recovery and reuse in order to reduce the costs of the biodiesel production  
222 process<sup>41</sup>. Therefore, after each reaction, the catalyst was washed with 3 mL of ethanol and dried in  
223 order to remove possible impurities that could affect the conversion<sup>42</sup>. The combi-lipase 25:75 SBA-  
224 15-NH<sub>2</sub>G-CalB:SBA-15-NH<sub>2</sub>G-PC was reused for 10 consecutive cycles under the same operating  
225 conditions (Figure 6).



226

227

**Figure 6.** Reuse of combi-lipase 25:75 SBA-15-NH<sub>2</sub>G-CalB:SBA-15-NH<sub>2</sub>G-PC.

228 The results showed that the conversion was above 80 mol% during the first five cycles,  
229 decreasing by 10% with respect to the first reaction. Subsequently, the conversion gradually  
230 decreased, reaching a conversion of around 70 mol% after the tenth reuse. These results are  
231 comparable although better than others reported in the literature for the lipase from *P. cepacia* where  
232 after the first use, 10% of the activity was lost and in the fourth cycle the activity was reduced by  
233 53%<sup>43</sup>. This loss of activity can be caused by a possible deterioration of the biocatalyst by enzyme  
234 poisoning<sup>44</sup>.

235

### 236 3. Materials and methods

#### 237 3.1. Microalga

238 The microalga used in this work was *Isochrysis galbana* and it was supplied by AlgaEnergy S.A.  
239 (Spain). This strain has been selected due to its high lipid content (33.5 wt%), which makes it favorable  
240 for the production of FAEEs.

#### 241 3.2. Lipid extraction

242 The extraction of lipids from the microalga, in the dry biomass procedure, was carried out with  
243 a dry microalga:solvent ratio of 1:20, using ethyl acetate as solvent. The samples were stirred  
244 vigorously with the help of a vortex (Finecorp, Korea) for 5 min at 11000 rpm at room temperature to  
245 obtain the lipids contained in the microalgae. In the case of the extraction of lipids from wet biomass,  
246 the same procedure was carried out starting from a suspension of microalga in water with a  
247 concentration of 50 g/L.

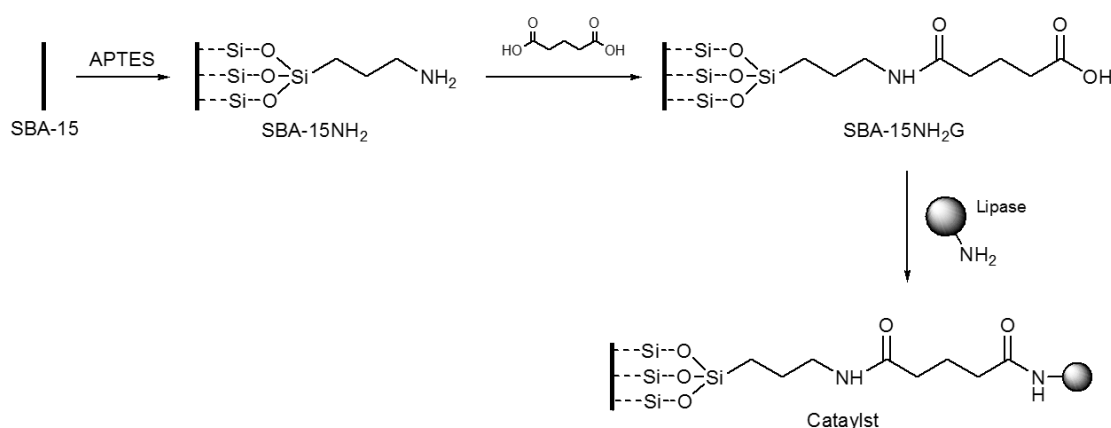
#### 248 3.3. Synthesis of lipase-based biocatalysts

249 The assays for the production of FAEEs were carried out using lipase B from *Candida antarctica*  
250 (CalB) and lipase from *Pseudomonas cepacia* (PC), both from Sigma-Aldrich (USA), supported on SBA-  
251 15 modified with amino groups and glutaraldehyde following protocols previously described<sup>45-47</sup>  
252 (Figure 7).

253 In a typical synthesis for SBA-15, 8 g of block copolymer surfactant Pluronic 123 (Sigma-Aldrich)  
254 were dissolved at room temperature under stirring in 250 mL of 1.9 M HCl (Scharlab, Spain). The  
255 solution was heated up to 40 °C and 17.8 g of TEOS (tetraethyl orthosilicate, Sigma-Aldrich) were  
256 added to the solution. The resultant mixture was then stirred at that temperature for 20 h and  
257 hydrothermally aged at 110 °C for further 24 h. The template was removed by calcination at 550 °C  
258 for 5 h at a heating rate of 1.8 °C/min<sup>46</sup>.

259 The protocol for covalent immobilization of lipases (Fig. 7) was adapted from Wang's  
260 procedure<sup>37</sup>. Thus, 2 g of calcined mesoporous material SBA-15 were immersed into a solution of 1 g  
261 of APTES (*n*-aminopropyltriethoxysilane, Sigma-Aldrich) in 30 mL of anhydrous toluene (Sigma-  
262 Aldrich). The mixture was refluxed at 110 °C for 24 h under inert nitrogen atmosphere. Then, the  
263 suspension was filtered and washed 3 times with anhydrous toluene. The solid was placed in glass  
264 vials and vacuum dried for 24 h at 110 °C, yielding the amine-functionalized support named SBA-15-  
265 NH<sub>2</sub>. Then, 1 g of SBA-15-NH<sub>2</sub> was blended with 1 mL of 25 vol% aqueous glutaraldehyde (Sigma-  
266 Aldrich) and 9 mL of 0.1 M phosphate buffer (Sigma-Aldrich) for 2 h. The solid material (SBA-15-  
267 NH<sub>2</sub>G) was filtered and washed with phosphate buffer.

268 The functionalized materials were used as carriers for lipase immobilization. 100 mg of amino-  
269 functionalized and glutaraldehyde linked mesoporous material was blended with 1 mL of lipase in  
270 4 mL of 0.1 M phosphate buffer at pH=7.0 and the mixture was shaken at 200 rpm and 25°C for 3 h.  
271 Then, the material was filtered and washed three times with 5 mL phosphate buffer. The final  
272 biocatalysts produced were named as SBA-15-NH<sub>2</sub>G-CalB and SBA-15-NH<sub>2</sub>G-PC, containing  
273 immobilized CalB and PC lipase, respectively.



274

275

**Figure 7.** Synthesis of the enzymatic catalyst supported on SBA-15

276

### 3.4. Characterization of biocatalysts

277

278

279

280

281

282

283

284

285

286

287

288

289

290

291

292

293

294

295

296

297

298

299

300

301

302

The evaluation of the textural properties of SBA-15 mesoporous materials was performed by N<sub>2</sub> adsorption/desorption isotherms in a Tristar model 3000 equipment (Micromeritics, USA). Prior to the analysis, a degasification stage is carried out based on the controlled heating of the samples up to 250°C and 120°C, for inorganic and organically functionalized samples, respectively, and the use of a nitrogen current in a SmartPrep type degasser. The specific surface area was calculated by the Brunauer-Emmett-Teller (BET) method, the pore diameter was measured through the Barret-Joyner-Halenda technique (BJH) and pore volume was determined by using the Harkins-Jura technique.

X-ray diffraction experiments were performed in a X'Pert MPD (Philips, The Netherlands) using monochromatic Cu K $\alpha$  radiation, with a wavelength of 1.54 Å. The step size was 0.02° with an accumulation time per step of 5 seconds for a sweep of angles 2 $\theta$  of 5–50°.

Transmission electron microscopy (TEM) analysis was performed with a Tecnai 20 microscope (Philips, The Netherlands) with a resolution of 0.27 nm and  $\pm 70^\circ$  inclination of the sample, equipped with an EDX detector.

<sup>29</sup>Si NMR spectroscopy allow to determine the relationship between condensed and non-condensed silicon species, obtaining structural information about the mesoporous siliceous material<sup>38</sup>. These experiments were performed in an Infinity AS400 NMR spectrometer (Varian, USA) operating at 9.4 Tesla.

The content of hydrogen, carbon, nitrogen, sulfur and oxygen was measured in a Vario EL III element analyzer (Elementar Analysensysteme GmbH, Germany) using sulphanic acid as standard.

To evaluate the thermal stability of the SBA-15 materials, thermogravimetric analysis (TGA) were carried out under inert atmosphere (nitrogen) in an 1100 TGA/DSC1 model (Mettler Toledo, USA). The thermal analysis ranged from 40°C to 800°C with a ramp of 10 °C/min.

Finally, the amount of enzyme immobilized was calculated by mass balance measuring the enzyme concentration in the supernatant solution using the Bradford's assay with bovine serum albumin (BSA) as standard<sup>48</sup>. All the analyses were performed in triplicate.

### 3.5. FAEEs production

303 FAEE production experiments were carried out in 12 mL glass pressure tubes (Sigma-Aldrich).  
304 0.1 g of extracted lipids, 2 mL of ethanol as solvent and 15 mg of the synthesized biocatalyst were  
305 employed<sup>11</sup>. The reaction mixture was maintained at 50°C and 300 rpm for 24 h. After the reaction  
306 time, the mixture was cooled to room temperature generating two liquid phases. The upper phase  
307 containing FAEE was washed twice with 10 mL of water and then with 10 mL of hexane:diethylether  
308 mixture (80:20). To carry out a comparative study, the commercial biocatalysts Novozym 435® (N345)  
309 was used. Conversion of saponifiable lipids into FAEEs was measured by <sup>1</sup>H-NMR analyses  
310 performed in a Varian Mercury Plus 400 unit, following the procedure reported in the literature<sup>49</sup>.

311 FAEE production reactions were also carried out using combi-lipase biocatalysts with the  
312 following SBA15-NH<sub>2</sub>G-CalB:SBA15-NH<sub>2</sub>G-PC ratios: 25:75, 50:50 and 75:25 wt%. Finally, successive  
313 reactions were carried out under the same conditions to assess the reuse capacity.

### 314 3.6. FAEE characterization

315 The characteristics of the FAEE to be used as biodiesel have to be evaluated based on the  
316 standard EN 14214, in which the protocol for determining the iodine value of the biodiesel obtained  
317 is included. In addition, the content of mono-, di- and triglycerides was determined by thin layer  
318 chromatography (TLC) following the method described by Vicente et al.<sup>2</sup>, where the sample was  
319 diluted with hexane. The TLC plate was developed, stained with iodine and digitized. The software  
320 Un-Scan-It Gel 6.1 (Silk Scientific Inc. USA) was used for the quantification of each lipid fraction using  
321 the corresponding standards. The non-saponifiable extracted matter was determined by a  
322 gravimetric procedure described elsewhere<sup>50</sup>.

323 The sulfur content was measured by elemental analysis in a Vario EL III elemental analyzer and  
324 metals were determined by inductively coupled plasma atomic emission spectroscopy in a Vista AX  
325 CCD simultaneous ICP-AES equipment coupled to a spectrophotometer (Varian Inc. Germany)  
326 following EN 14538 (for Na, K, Ca and Mg) and EN 14107 (for P) standards, respectively.

## 327 4. Conclusions

328 Lipids from *Isochrysis galbana* extracted with ethyl acetate using both dry and wet biomass were  
329 used to produce biodiesel (FAEEs) with heterogeneous lipase-based biocatalysts. Lipase B from  
330 *Candida antarctica* (CalB) and lipase from *Pseudomonas cepacia* (PC) were covalently immobilised on  
331 amino-functionalised SBA-15. Their catalytic activity was compared with that of the commercial  
332 catalyst Novozym 435. The conversion to FAEEs using the synthesized biocatalysts SBA-15-NH<sub>2</sub>G-  
333 CalB (97 and 85.5 mol% for dry and wet extraction, respectively) and SBA-15-NH<sub>2</sub>G-PC (91 and 87  
334 mol%) resulted in higher conversions for both dry and wet ones than those obtained with the  
335 commercial catalyst N435 (75 and 69.5 mol%). Due to the heterogeneous nature of the lipid  
336 composition of the microalgae, mixtures with different proportions of CALB:PC biocatalysts were  
337 used to improve the conversion of wet extracted lipids. The results showed that a combi-lipase  
338 biocatalyst 25:75 SBA-15-NH<sub>2</sub>G-CalB:SBA-15-NH<sub>2</sub>G-PC produced a conversion of FAEE (97.2 mol%)  
339 significantly higher than those produced from wet extracted oil by biocatalysts containing a single  
340 lipase and similar to the maximum conversion using oils from wet extraction. Therefore, the combi-  
341 lipase presented can help to improve the viability of a microalgal biorefinery since the biomass-  
342 drying step can be avoided for biodiesel production.

343 **Author Contributions:** ASB performed the experimental work (synthesis of biocatalysts, catalytic experiments  
344 and sample characterization) and made a first draft of the manuscript. VM and RR analyzed and discussed the  
345 results of biocatalysts characterization and VM collaborated in the writing of the first draft of the manuscript.  
346 FB and GV devised the experimental work, analyzed the catalytic tests and wrote the final version of the  
347 manuscript. The listed authors have contributed substantially to this work.

348 **Funding:** The authors acknowledge the financial support from the projects S2013/ABI-2783 (Comunidad de  
349 Madrid y FEDER “Una manera de hacer Europa”) and CTQ2013-44447-R (Ministerio de Economía y  
350 Competitividad).

351 **Conflicts of Interest:** The authors declare no conflict of interest.

## 352 References

- 353 (1) Demirbas, A. Political, Economic and Environmental Impacts of Biofuels: A Review. *Appl.*  
354 *Energy* **2009**, *86*, S108–S117. <https://doi.org/10.1016/j.apenergy.2009.04.036>.
- 355 (2) Vicente, G.; Bautista, L. F.; Rodríguez, R.; Gutiérrez, F. J.; Sádaba, I.; Ruiz-Vázquez, R. M.;  
356 Torres-Martínez, S.; Garre, V. Biodiesel Production from Biomass of an Oleaginous Fungus.  
357 *Biochem. Eng. J.* **2009**, *48* (1), 22–27. <https://doi.org/10.1016/j.bej.2009.07.014>.
- 358 (3) Carrero, A.; Vicente, G.; Rodríguez, R.; Peso, G. L. del; Santos, C. Synthesis of Fatty Acids  
359 Methyl Esters (FAMEs) from *Nannochloropsis gaditana* Microalga Using Heterogeneous Acid  
360 Catalysts. *Biochem. Eng. J.* **2015**, *97*, 119–124. <https://doi.org/10.1016/j.bej.2015.02.003>.
- 361 (4) Bautista, L. F.; Vicente, G.; Mendoza, Á.; González, S.; Morales, V. Enzymatic Production of  
362 Biodiesel from *Nannochloropsis gaditana* Microalgae Using Immobilized Lipases in  
363 Mesoporous Materials. *Energy and Fuels* **2015**, *29* (8), 4981–4989.  
364 <https://doi.org/10.1021/ef502838h>.
- 365 (5) Guldhe, A.; Singh, B.; Mutanda, T.; Permaul, K.; Bux, F. Advances in Synthesis of Biodiesel  
366 via Enzyme Catalysis: Novel and Sustainable Approaches. *Renew. Sustain. Energy Rev.* **2015**,  
367 *41*, 1447–1464. <https://doi.org/10.1016/j.rser.2014.09.035>.
- 368 (6) Navarro López, E.; Robles Medina, A.; Esteban Cerdán, L.; González Moreno, P. A.; Macías  
369 Sánchez, M. D.; Molina Grima, E. Fatty Acid Methyl Ester Production from Wet Microalgal  
370 Biomass by Lipase-Catalyzed Direct Transesterification. *Biomass and Bioenergy* **2016**, *93*, 6–12.  
371 <https://doi.org/10.1016/j.biombioe.2016.06.018>.
- 372 (7) Park, J.-Y.; Park, M. S.; Lee, Y.-C. Advances in Direct Transesterification of Algal Oils from  
373 Wet Biomass. *Bioresour. Technol.* **2015**, *184*, 267–275.  
374 <https://doi.org/10.1016/j.biortech.2014.10.089>.
- 375 (8) Dalla-Vecchia, R.; Nascimento, M. D. G.; Soldi, V. Aplicações Sintéticas de Lipases  
376 Imobilizadas Em Polímeros. *Quim. Nova* **2004**, *27* (4), 623–630. <https://doi.org/10.1590/S0100-40422004000400017>.
- 377 (9) Hanefeld, U.; Gardossi, L.; Magner, E. Understanding Enzyme Immobilisation. *Chem. Soc.*  
378 *Rev.*; 2009; Vol. 38. <https://doi.org/10.1039/b711564b>.
- 379 (10) Rios, N. S.; Pinheiro, M. P.; dos Santos, J. C. S.; de S. Fonseca, T.; Lima, L. D.; de Mattos, M. C.;  
380 Freire, D. M. G.; da Silva, I. J.; Rodríguez-Aguado, E.; Gonçalves, L. R. B. Strategies of Covalent  
381 Immobilization of a Recombinant *Candida antarctica* Lipase B on Pore-Expanded SBA-15 and  
382 Its Application in the Kinetic Resolution of (R,S)-Phenylethyl Acetate. *J. Mol. Catal. B Enzym.*  
383 **2016**, *133*, 246–258. <https://doi.org/10.1016/j.molcatb.2016.08.009>.
- 384 (11) Bautista, L. F.; Vicente, G.; Mendoza, Á.; González, S.; Morales, V. Enzymatic Production of  
385 Biodiesel from *Nannochloropsis gaditana* Microalgae Using Immobilized Lipases in  
386

- 387 Mesoporous Materials. *Energy and Fuels* **2015**, *29* (8), 4981–4989.  
388 <https://doi.org/10.1021/ef502838h>.
- 389 (12) Abdullah, A. Z. Z.; Sulaiman, N. S. S.; Kamaruddin, A. H. H. Biocatalytic Esterification of  
390 Citronellol with Lauric Acid by Immobilized Lipase on Aminopropyl-Grafted Mesoporous  
391 SBA-15. *Biochem. Eng. J.* **2009**, *44* (2–3), 263–270. <https://doi.org/10.1016/j.bej.2009.01.007>.
- 392 (13) Canilho, N.; Jacoby, J.; Pasc, A.; Carteret, C.; Dupire, F.; Stébé, M. J.; Blin, J. L. Isocyanate-  
393 Mediated Covalent Immobilization of *Mucor miehei* Lipase onto SBA-15 for Transesterification  
394 Reaction. *Colloids Surf. B. Biointerfaces* **2013**, *112*, 139–145.  
395 <https://doi.org/10.1016/j.colsurfb.2013.07.024>.
- 396 (14) Zhou, Z.; Piepenbreier, F.; Marthala, V. R. R.; Karbacher, K.; Hartmann, M. Immobilization of  
397 Lipase in Cage-Type Mesoporous Organosilicas via Covalent Bonding and Crosslinking.  
398 *Catal. Today* **2015**, *243* (C), 173–183. <https://doi.org/10.1016/j.cattod.2014.07.047>.
- 399 (15) Zniszczoł, A.; Herman, A. P.; Szymańska, K.; Mrowiec-Białoń, J.; Walczak, K. Z.; Jarzebski, A.;  
400 Boncel, S. Covalently Immobilized Lipase on Aminoalkyl-, Carboxy- and Hydroxy-Multi-  
401 Wall Carbon Nanotubes in the Enantioselective Synthesis of Solketal Esters. *Enzyme Microb.*  
402 *Technol.* **2016**, *87–88*, 61–69. <https://doi.org/10.1016/j.enzmictec.2016.02.015>.
- 403 (16) Dhawane, S. H.; Kumar, T.; Halder, G. Recent Advancement and Prospective of  
404 Heterogeneous Carbonaceous Catalysts in Chemical and Enzymatic Transformation of  
405 Biodiesel. *Energy Convers. Manag.* **2018**, *167*, 176–202.  
406 <https://doi.org/10.1016/J.ENCONMAN.2018.04.073>.
- 407 (17) Rios, N. S.; Pinheiro, M. P.; Lima, M. L. B.; Freire, D. M. G.; da Silva, I. J.; Rodríguez-Castellón,  
408 E.; de Sant’Ana, H. B.; Macedo, A. C.; Gonçalves, L. R. B. Pore-Expanded SBA-15 for the  
409 Immobilization of a Recombinant *Candida antarctica* Lipase B: Application in Esterification and  
410 Hydrolysis as Model Reactions. *Chem. Eng. Res. Des.* **2018**, *129*, 12–24.  
411 <https://doi.org/10.1016/j.cherd.2017.10.032>.
- 412 (18) Ashjari, M.; Mohammadi, M.; Badri, R. Selective Concentration of Eicosapentaenoic Acid and  
413 Docosahexaenoic Acid from Fish Oil with Immobilized/Stabilized Preparations of *Rhizopus*  
414 *oryzae* Lipase. *J. Mol. Catal. B Enzym.* **2015**, *122*, 147–155.  
415 <https://doi.org/10.1016/j.molcatb.2015.08.017>.
- 416 (19) Lee, J. S.; Yim, J. H.; Jeon, J. K.; Ko, Y. S. Polymerization of Olefins with Single-Site Catalyst  
417 Anchored on Amine-Functionalized Surface of SBA-15. *Catal. Today* **2012**, *185* (1), 175–182.  
418 <https://doi.org/10.1016/j.cattod.2011.12.003>.
- 419 (20) Yiu, H. H. P.; Wright, P. A.; Botting, N. P. Enzyme Immobilisation Using SBA-15 Mesoporous  
420 Molecular Sieves with Functionalised Surfaces. *J. Mol. Catal. Enzym.* **2001**, *15* (1–3), 81–92.  
421 [https://doi.org/10.1016/S1381-1177\(01\)00011-X](https://doi.org/10.1016/S1381-1177(01)00011-X).
- 422 (21) Tongboriboon, K.; Cheirsilp, B.; H-Kittikun, A. Mixed Lipases for Efficient Enzymatic  
423 Synthesis of Biodiesel from Used Palm Oil and Ethanol in a Solvent-Free System. *J. Mol. Catal.*  
424 *B Enzym.* **2010**, *67* (1–2), 52–59. <https://doi.org/10.1016/J.MOLCATB.2010.07.005>.
- 425 (22) Guldhe, A.; Singh, B.; Rawat, I.; Permaul, K.; Bux, F. Biocatalytic Conversion of Lipids from  
426 Microalgae *Scenedesmus Obliquus* to Biodiesel Using *Pseudomonas fluorescens* Lipase. *Fuel* **2015**,  
427 *147*, 117–124. <https://doi.org/10.1016/J.FUEL.2015.01.049>.
- 428 (23) He, Y.; Wu, T.; Wang, X.; Chen, B.; Chen, F. Cost-Effective Biodiesel Production from Wet  
429 Microalgal Biomass by a Novel Two-Step Enzymatic Process. *Bioresour. Technol.* **2018**, *268*,

- 430 583–591. <https://doi.org/10.1016/J.BIORTECH.2018.08.038>.
- 431 (24) Guldhe, A.; Singh, P.; Renuka, N.; Bux, F. Biodiesel Synthesis from Wastewater Grown  
432 Microalgal Feedstock Using Enzymatic Conversion: A Greener Approach. *Fuel* **2019**, *237*,  
433 1112–1118. <https://doi.org/10.1016/J.FUEL.2018.10.033>.
- 434 (25) Bauer, G.; Lima, S.; Chenevard, J.; Sugnaux, M.; Fischer, F. Biodiesel via in Situ Wet Microalgae  
435 Biotransformation: Zwitter-Type Ionic Liquid Supported Extraction and Transesterification.  
436 **2017**. <https://doi.org/10.1021/acssuschemeng.6b02665>.
- 437 (26) Castillo López, B.; Esteban Cerdán, L.; Robles Medina, A.; Navarro López, E.; Martín  
438 Valverde, L.; Hita Peña, E.; González Moreno, P. A.; Molina Grima, E. Production of Biodiesel  
439 from Vegetable Oil and Microalgae by Fatty Acid Extraction and Enzymatic Esterification. *J.*  
440 *Biosci. Bioeng.* **2015**, *119* (6), 706–711. <https://doi.org/10.1016/J.JBIOOSC.2014.11.002>.
- 441 (27) Banerjee, A.; Singh, V.; Solanki, K.; Mukherjee, J.; Gupta, M. Combi-Protein Coated  
442 Microcrystals of Lipases for Production of Biodiesel from Oil from Spent Coffee Grounds.  
443 *Sustain. Chem. Process.* **2013**, *1* (1), 14. <https://doi.org/10.1186/2043-7129-1-14>.
- 444 (28) Alves, J. S.; Vieira, N. S.; Cunha, A. S.; Silva, A. M.; Záchia Ayub, M. A.; Fernandez-Lafuente,  
445 R.; Rodrigues, R. C. Combi-Lipase for Heterogeneous Substrates: A New Approach for  
446 Hydrolysis of Soybean Oil Using Mixtures of Biocatalysts. *RSC Adv.* **2014**, *4* (14), 6863–6868.  
447 <https://doi.org/10.1039/C3RA45969A>.
- 448 (29) Bajaj, A.; Lohan, P.; Jha, P. N.; Mehrotra, R. Biodiesel Production through Lipase Catalyzed  
449 Transesterification: An Overview. *J. Mol. Catal. B Enzym.* **2010**, *62* (1), 9–14.  
450 <https://doi.org/10.1016/J.MOLCATB.2009.09.018>.
- 451 (30) Lee, H. W.; Cho, H. J.; Yim, J. H.; Kim, J. M.; Jeon, J. K.; Sohn, J. M.; Yoo, K. S.; Kim, S. S.; Park,  
452 Y. K. Removal of Cu(II)-Ion over Amine-Functionalized Mesoporous Silica Materials. *J. Ind.*  
453 *Eng. Chem.* **2011**, *17* (3), 504–509. <https://doi.org/10.1016/j.jiec.2010.09.022>.
- 454 (31) Serra, E.; Mayoral, Á.; Sakamoto, Y.; Blanco, R. M.; Díaz, I. Immobilization of Lipase in  
455 Ordered Mesoporous Materials: Effect of Textural and Structural Parameters. *Microporous*  
456 *Mesoporous Mater.* **2008**, *114* (1–3), 201–213. <https://doi.org/10.1016/j.micromeso.2008.01.005>.
- 457 (32) Sun, Q.; Fu, C. W.; Aguila, B.; Perman, J.; Wang, S.; Huang, H. Y.; Xiao, F. S.; Ma, S. Pore  
458 Environment Control and Enhanced Performance of Enzymes Infiltrated in Covalent Organic  
459 Frameworks. *J. Am. Chem. Soc.* **2018**, *140* (3), 984–992. <https://doi.org/10.1021/jacs.7b10642>.
- 460 (33) Rabbani, G.; Ahmad, E.; Khan, M. V.; Ashraf, M. T.; Bhat, R.; Khan, R. H. Impact of Structural  
461 Stability of Cold Adapted *Candida antarctica* Lipase B (CaLB): In Relation to pH, Chemical and  
462 Thermal Denaturation. *RSC Adv.* **2015**, *5* (26), 20115–20131.  
463 <https://doi.org/10.1039/C4RA17093H>.
- 464 (34) Gómez-Orozco, S. Y.; Huirache-Acuña, R.; Pawelec, B.; Fierro, J. L. G.; Rivera-Muñoz, E. M.;  
465 Lara-Romero, J.; Alonso-Nuñez, G. Characterizations and HDS Performances of Sulfided  
466 NiMoW Catalysts Supported on Mesoporous Titania-Modified SBA-15. *Catal. Today* **2018**, *305*,  
467 152–161. <https://doi.org/10.1016/j.cattod.2017.08.009>.
- 468 (35) Mohammadi M.; Habibi, Z.; Gandomkar, S.; Yousefi, M. A Novel Approach for  
469 Bioconjugation of *Rhizomucor Miehei* Lipase (RML) onto Amine-Functionalized Supports;  
470 Application for Enantioselective Resolution of Rac-Ibuprofen. *Int. J. Biol. Macromol.* **2018**.  
471 <https://doi.org/10.1016/j.procbio.2018.02.010>.
- 472 (36) Zhao, X. S.; Lu, G. Q.; Whittaker, A. K.; G. J. Millar, A.; Zhu, H. Y. Comprehensive Study of

- 473 Surface Chemistry of MCM-41 Using  $^{29}\text{Si}$  CP/MAS NMR, FTIR, Pyridine-TPD, and TGA. *J.*  
474 *Phys. Chem. B* **1997**, *33*, 6525–6531. <https://doi.org/10.1021/JP971366+>.
- 475 (37) Wang, C.; Zhou, G.; Li, Y.-J.; Lu, N.; Song, H.; Zhang, L. Biocatalytic Esterification of Caprylic  
476 Acid with Caprylic Alcohol by Immobilized Lipase on Amino-Functionalized Mesoporous  
477 Silica. *Colloids Surfaces A Physicochem. Eng. Asp.* **2012**, *406*, 75–83.  
478 <https://doi.org/10.1016/J.COLSURFA.2012.04.053>.
- 479 (38) Simonutti, R.; Comotti, A.; Bracco, S.; Sozzani, P. Surfactant Organization in MCM-41  
480 Mesoporous Materials As Studied by  $^{13}\text{C}$  and  $^{29}\text{Si}$  Solid-State NMR. *Chem. Mater.* **2001**, *13* (3),  
481 771–777. <https://doi.org/10.1021/cm001088i>.
- 482 (39) Guncheva, M.; Yancheva, D.; Ossowicz, P.; Janus, E. Structural Basis for the Inactivation of  
483 *Candida rugosa* Lipase in the Presence of Amino Acid Ionic Liquids. *Bulg. Chem. Commun.* **2017**,  
484 *49*, 132–136.
- 485 (40) Alves, J.; S. Vieira, N.; S. Cunha, A.; M. Silva, A.; Ayub, M.; Fernandez-Lafuente, R.; Rodrigues,  
486 R. Combi-Lipase for Heterogeneous Substrates: A New Approach for Hydrolysis of Soybean  
487 Oil Using Mixtures of Biocatalysts. *RSC Adv.* **2014**, *4*, 6863–6868.  
488 <https://doi.org/10.1039/c3ra45969a>.
- 489 (41) Amini, Z.; Ilham, Z.; Ong, H. C.; Mazaheri, H.; Chen, W.-H. State of the Art and Prospective  
490 of Lipase-Catalyzed Transesterification Reaction for Biodiesel Production. *Energy Convers.*  
491 *Manag.* **2017**, *141*, 339–353. <https://doi.org/10.1016/j.enconman.2016.09.049>.
- 492 (42) Galgali, A.; Gawas, S. D.; Rathod, V. K. Ultrasound Assisted Synthesis of Citronellol Laurate  
493 by Using Novozym 435. *Catal. Today* **2018**, *309*, 133–139.  
494 <https://doi.org/10.1016/j.cattod.2017.08.052>.
- 495 (43) Piligaev, A. V.; Sorokina, K. N.; Samoylova, Y. V.; Parmon, V. N. Lipid Production by  
496 Microalga *Micractinium* Sp. IC-76 in a Flat Panel Photobioreactor and Its Transesterification  
497 with Cross-Linked Enzyme Aggregates of *Burkholderia cepacia* Lipase. *Energy Convers. Manag.*  
498 **2018**, *156* (August 2017), 1–9. <https://doi.org/10.1016/j.enconman.2017.10.086>.
- 499 (44) Navarro López, E.; Robles Medina, A.; González Moreno, P. A.; Esteban Cerdán, L.; Martín  
500 Valverde, L.; Molina Grima, E. Biodiesel Production from *Nannochloropsis gaditana* Lipids  
501 through Transesterification Catalyzed by *Rhizopus oryzae* Lipase. *Bioresour. Technol.* **2016**,  
502 *203*, 236–244. <https://doi.org/10.1016/j.biortech.2015.12.036>.
- 503 (45) Lai, J. Q.; Hu, Z. L.; Wang, P. W.; Yang, Z. Enzymatic Production of Microalgal Biodiesel in  
504 Ionic Liquid [BMIm][PF 6]. *Fuel* **2012**, *95*, 329–333. <https://doi.org/10.1016/j.fuel.2011.11.001>.
- 505 (46) Zhao, D.; Feng, J.; Huo, Q.; Melosh, N.; Glenn, H.; Chmelka, B. F.; Stucky, G. D.; Zhao, D.;  
506 Feng, J.; Huo, Q.; et al. Triblock Copolymer Syntheses of Mesoporous Silica with Periodic  
507 to 300 Angstrom. *Science (80-. )*. **1998**, *279* (5350), 548–552.
- 508 (47) Salis, A.; Pinna, M.; Monduzzi, M.; Solinas, V. Biodiesel Production from Triolein and Short  
509 Chain Alcohols through Biocatalysis. *J. Biotechnol.* **2005**, *119* (3), 291–299.  
510 <https://doi.org/10.1016/j.jbiotec.2005.04.009>.
- 511 (48) Bradford, M. M. A Rapid and Sensitive Method for the Quantitation of Microgram Quantities  
512 of Protein Utilizing the Principle of Protein-Dye Binding. *Anal. Biochem.* **1976**, *72* (1–2), 248–  
513 254. [https://doi.org/10.1016/0003-2697\(76\)90527-3](https://doi.org/10.1016/0003-2697(76)90527-3).
- 514 (49) Jaiswal, S. K.; Tejo Prakash, N.; Prakash, R.  $^1\text{H}$  NMR Based Quantification of  $^1\text{H}$  NMR Based  
515 Quantification of Ethyl Ester in Biodiesel: A Comparative Study of Product-Dependent

516 Derivations. *Anal. Chem. Lett.* **2016**, *6* (5), 518–525.  
517 <https://doi.org/10.1080/22297928.2016.1246977>.  
518 (50) Panreac Quimica, S. . *Métodos Analíticos En Alimentaria*; 1999.  
519